Mass Transfer in a Wetted-wall Column: Turbulent Flow

W. H. SCHWARZ and H. E. HOELSCHER

The Johns Hopkins University, Baltimore, Maryland

The object of this study has been the measurement of concentration profiles of water vapor in a wetted-wall column with fully developed turbulent pipe flow of air for several positions downstream of the inlet. The air Reynolds number was 25,000. The mathematical formulation of this problem involves the Navier-Stokes equations and the mass transfer equation with a boundary condition of constant concentration at the wall. No attempt has been made toward an analytical solution of this problem, as the exact solution of the turbulence problem has not been developed. Instead, values of the mass and momentum transfer correlation, $\overline{u_r h}$ and $\overline{u_r u_z}$, have been computed as a function of the radius. The eddy diffusivity for momentum and mass and the local mass transfer rates are shown for engineering purposes.

In the past, investigators of the wetted-wall column have been interested only in the measurement of over-all mass transfer coefficients of a liquid evaporating into the air or in its analogous problem, a chemical contaminent being absorbed into the liquid. These over-all mass transfer coefficients were correlated by the use of dimensionless groups (*17*). Considerable discrepancy has been found in the experimental results.

Obviously the measurement of the gross properties of a system does not give an insight into the mechanisms of the transport of mass into a turbulent gas stream. More meaningful information can be obtained by the measurement of mean concentration profiles, especially when coupled with the detailed statistical information of Laufer (*10*) on the turbulent flow of air in a round duct.

From measurements of the mean velocity and concentration profiles, distributions of momentum and mass transport coefficients are directly calculable. However, it has been found that the mean profile is relatively insensitive to phenomenological assumptions on the transfer coefficient, and so direct experimental determination of the local transfer rates would be desirable and could presumably be obtained by the use of the hot-wire anemometer, giving direct measurement of statistical correlation such as $\overline{u_r h} \sim$ the concentration diffusion, concentration fluctuation level h/H, the spectrum of concentration scale, and microscale. Having these statistical properties will allow partial solution of other types of shear flows where the properties of the flow field are known. Although theory has been developed for the hot-wire anemometer for the purpose of these measurements (*1*), it has apparently never been applied to mass transfer problems. It is logical, therefore, that the next step would be the development of the hot wire for this purpose and its application to the turbulent mass transfer problem.

There are few experimental data in the literature pertaining to wetted-wall columns where conditions have been defined satisfactorily and the properties measured to ensure reproducibility of results. Most of the difficulty stems from the lack of the fully developed state of the flow, the poor choice of measurement techniques, and failure to consider the effect of the development of the concentration profile.

Probably the most reliable wetted-wall data for evaporation of liquids into a turbulent air stream is the work of Gilliland and Sherwood (*5*). However, only over-all measurements of the mean outlet and inlet concentrations and temperatures were made. No rippling effects were noted.

Linton and Sherwood (*11*) noted the effect of the length of tube-to-diameter ratio on the mass transfer coefficient. An excellent review of the methods of correlation and a listing of other references are found in an article by Sherwood and Pigford (*17*). Mixing-length theories are discussed in several articles (*6, 13, 15*).

The information gained from this problem is fundamental in many applications to reactors, absorption towers, and numerous other unit operations involving the transfer of material. They are all concerned with the basic mass transfer differential equation. From the concentration profiles, transport coefficients may be measured which, combined with the mixing-length theory, offer engineering solutions to other problems where the flow conditions are similar.

DESCRIPTION OF EQUIPMENT

Operational Equipment

The wetted-wall column was constructed from a standard Pyrex-glass tube (3.33 in. I.D.) 4 ft. in length. The top edge was ground flat so that the liquid flowing over the edge would be distributed uniformly around the periphery, and the bottom edge was flared into a 30° angle (about 2 in. long) so that the liquid might be removed from the column. The liquid was fed into the upper calming section of the column from a 5-gal. constant-head tank. This tank was connected into a recycling system. A constant liquid-supply temperature was maintained by regulating the current on a heater in the constant-head tank. The water fed into the calming section was metered by a calibrated Fischer and Porter rotameter. This liquid was introduced into the calming section through a length of ⅜-in. copper tubing. Holes of varying size and spacing were drilled in the tubing in order to achieve a uniform distribution in the upper section. A schematic diagram of the apparatus is shown in Figure 1.

The liquid was drawn from the column at the flared end of the tube into a removal section, where it was returned to the recycling system. A swing arm was built into the return line in order to maintain a constant level of liquid in the removal section.

The air was supplied by a 1-hp. centrifugal fan the speed of which was controlled by a rheostat. The fan had a 10- by 10-in. outlet leading into a tunnel which had 16-mesh screens properly spaced to reduce velocity fluctuations from the blower. It was necessary, owing to insufficient head room, to have the blower and tunnel on a horizontal plane and, therefore, to provide a right angle in the system. In order to minimize deleterious velocity perturbations and vortexes created by a right angle, a vane cascade was built. The vanes were constructed from sheet metal and were built in the shape of a single quadrant of a circle with two tangential pieces in the manner suggested by Pankhurst (*14*). The gap to chord ratio was 0.25; the chord was 3.17 in. radius 2.24 in.; the ratio of the radius to trailing edge was 6.32; and fifteen vanes were used in the cascade.

After the right-angled bend the air passed through a screen into a contraction which had a twofold purpose; it acted both as a contraction and as a section going from a square to a circular cross section. The contraction was made from plaster-of-Paris-impregnated gauze, reinforcing wire, and plaster of Paris. It was cast on a form constructed from sheet metal and a block of wood which was turned down on a lathe into the wide-bottomed-bell contraction shape. The inside of the contraction was sanded smooth and lacquered. The contraction area ratio was 10 to 1.

The contraction was coupled to a brass pipe, approximately 8 ft. in length, in which fine sand was glued to a 7-in. length of the walls at the entrance section to hasten transition from laminar to turbulent flow and to increase the rate of growth of the boundary layer. The brass pipe was beveled on the outer surface of the top to a 60° angle, in order to ensure a smooth fit with the tapered glass section.

The whole system was carefully aligned in the vertical direction by means of a carpenter's level and plumb bob. This was very important in obtaining smooth flow of liquid down the walls of the tube.

Measuring Equipment

The air flowing up through the column was sampled in ten places simultaneously over the cross section by means of multiple probe. This probe was constructed of a 4-ft. length of 3/8-in. brass tubing through which were inserted ten sections of 18/8-16 gauge stainless steel hypodermic tubing. At the outlet end of the brass tube each piece of hypodermic tubing was bent through two right angles so as to orient each sampling tube along the axis of the support tube but displaced from it by a predetermined amount. In cross section the probe assembly resembled a pitchfork, but the prongs, being the hypodermic sampling tubes, were located in two dimensions instead of one and were spaced over the cross section of the column so that relatively more samples were taken near the wall than in the center.

The 3/8-in. brass tube containing the hypodermic sampling tubes was mounted in a traversing gear movable in three directions. The sampling probe was carefully aligned in the column by use of the two horizontal adjustments on the traversing gear and was thence raised or lowered vertically by means of the third adjustment to any desired measurement point.

Each of the sampling tubes was connected through a separate capillary flow meter to a drying tube containing commercial Drierite. A vacuum pump and a control needle valve permitted the sampling rate to be adjusted so that the velocity through the sampling tube equaled the air velocity at the corresponding sampling point in the column. A by-pass connection around each drying tube permitted adjustment of the flows prior to actual measurement.

A by-pass *T* was located in each sampling line near the probe inlet and was connected to a Meriam micromanometer. This manometer could be read to approximately 0.0001 in. of water. In this manner the velocity distribution in the column was obtained from the total head reading.

Each of the ten capillary flow meters was calibrated by means of a wet-test meter whose calibration was checked by a water-displacement method.

The temperatures of the inlet and outlet water and air streams were measured by copper-constantan thermocouples and a Rubicon potentiometer accurate to ±2 μv. The temperatures were correct to ±0.2°F.

The drying tubes were weighed on a Becker chainomatic balance which read to 0.1 mg. To compensate for external addition or subtraction of weight by surface moisture, the U tubes were counterbalanced by a similar U tube during the weighing operation.

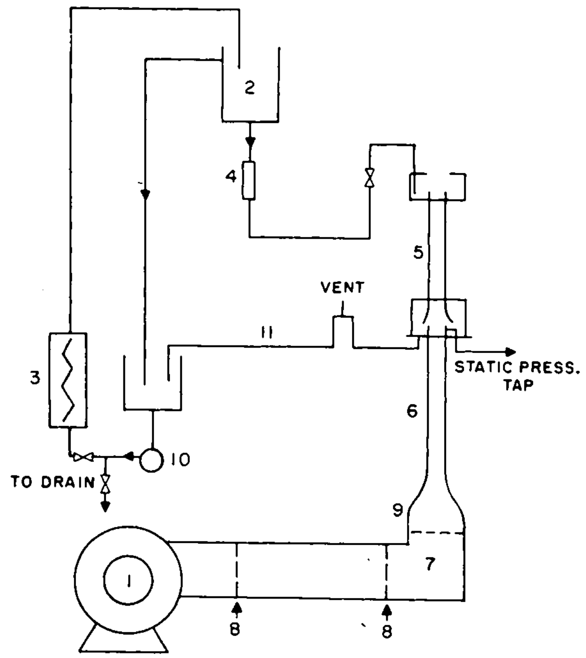

Fig. 1. Apparatus: 1, blower; 2, constant-head tank; 3, heater; 4, rotameter; 5, wetted-wall column glass section; 6, calming section (copper tube); 7, vanes; 8, screens, 9, contraction section; 10, recycle pump; 11, swing arm.

TABLE 1. VELICITY DISTRIBUTION

	Run 1	Run 2	Short tube	
y/a	U/U_{max}	U/U_{max}	y/a	U/U_{max}
1	1	1	1	1
0.8619	0.9894	0.9930	0.887	0.9973
0.7022	0.9763	0.951	0.768	0.9834
0.6027	0.9409	0.954	0.649	0.9504
0.5063	0.9022	0.9229	0.530	0.9166
0.375	0.8484	0.8576	0.411	0.8609
0.2724	0.8149	0.8032	0.292	0.8200
0.1989	0.7539	0.7764	0.1732	0.7599
0.1235	0.7171	0.6973	0.0541	0.6448
0.0603	0.6371	0.6526		

EXPERIMENTAL PROCEDURE

Water was added to the circulating system and brought to temperature. To this was added sufficient detergent (commercial Alconox) to make a 0.3% (weight) solution. The blower was turned on and adjusted to provide a flow of air equivalent to a Reynolds number of 25,000. All U tubes were weighed and mounted in place. The velocity head in the center of the tube was determined by the micromanometer and, from this U_{max} was calculated. From Figure 2, the velocity at the positions of the various sampling tubes was calculated. This velocity coupled with the area of the hypodermic tubing and specific volume of air per pound of dry air gave the flow rate in pounds per second to be drawn through each sampling tube. The capillary-flow-meter calibration charts gave the propér sampling flow rate at each point. All the needle valves were adjusted and the flow was switched from the by-pass to the U tubes. The air-flow rate was maintained at the desired level during the run. After a run of 2 hr. the tubes were reweighed to determine the moisture pickup.

EXPERIMENTAL MEASUREMENTS AND CORRECTIONS

In mass transfer operations a careful knowledge of the transfer surface is necessary. One of the inherent problems of the wetted-wall column is the difficulty of obtaining a smooth film. Rippling is always present, causing uncertainty in the measurement of the interfacial area. By the addition of small amounts of detergent to the water, rippling is eliminated. The water film was virtually undetectable upon visual observation. It was found that the optimum concentration of wetting agent (commercial Alconox) was 0.3% for the best smoothness at the operating range used. This result agrees closely with the work of Emmert and Pigford (*3*).

The air Reynolds number was fixed at 25,000 in order that the velocity be sufficiently high to give measurable total head readings, but low enough to have negligible effect upon the liquid surface. The liquid flow rate was set to obtain the smoothest film. Too low a liquid flow rate produced low-frequency and high-amplitude waves; whereas high flow rates gave high-frequency, low-amplitude waves.

The presence of the wetting agent on the evaporation of the liquid suggested that an equilibrium interfacial condition might not exist. Emmert and Pigford (*3*) determined that the wetting agent has little effect upon the assumed boundary condition at the interface, that of equilibrium with the film. Also, from the calculations of Schrage (*16*) using the data of Gilliland, it is shown that the interfacial resistance for this operation is negligible. Therefore, in a study of evaporation from a wetted-wall column of this type, the boundary condition of saturated water vapor at the wall seems justifiable.

The total head readings were all corrected for the velocity gradient by use of the method of Young and Maas (*19*). The empirical formula $E = 0.131e_1 + 0.082e_2$ was used to find the displacement of the probe to obtain its relative position in the tube. It was found on computation of the Reynolds number, based on the diameter of the probe, that the correction for viscous effects on the total head reading was negligible (*7, 12*).

The velocity traverse was taken by the probe used in sampling the air. The static pressure was measured by a small tap in the brass pipe slightly below the glass section. The static pressure at the probe was calculated from the linearity of the pressure drop with distance down the column. From these readings the velocity head was determined.

The velocity distribution measured with liquid flowing down the walls was not different from the distribution determined with a dry column within the limits of experimental error. In order to determine the effect of the joint between the brass pipe and glass tube, a small glass section 5 in. long was made and assembled into place. A velocity traverse across the open end was not discernibly different from that further downstream. The velocity profile across the open end of the brass pipe was also measured. Again the results were the same. Rotation of the probe gave a velocity traverse which was the same within experimental error. Thus the existence of fully developed turbulent flow was assured. It also showed that, although the interface velocity was not zero (*see below*), it was small enough to have negligible effect on the gas-flow field.

The velocity profile plotted as U/U_{max} vs. r/a is shown in Figure 2 and compared with the data of Laufer (*10*) for a Reynolds number of 50,000.

When the concentration profile was measured, no correction was used to determine a relative position of the probe, as was used to map the velocity field, since there is a reversal of signs of the velocity gradient (dU/dr) and concentration gradient (dH/dr). Thus the portion of the probe receiving the higher velocity was receiving a lower concentration and the part of the probe receiving a lower velocity was receiving a higher concentration of water vapor. The two effects will tend to cancel each other and the relative position probably matched the actual position very closely.

The velocity of the sample being sucked through the tubing was adjusted to the velocity of the air at the point of location. Corrsin (*2*), by an approximate analysis, has shown the error to be as high as 8% by letting only the head pressure of the air do the work in obtaining a sample and applying no suction.

An estimate of the liquid velocity was experimentally determined by spreading a powder on the liquid film and timing its movement over a measured distance. The maximum speed at the interface from many runs for the system used was 0.963 ft./sec. This allowed calculation of the liquid film thickness, which was 0.0050 in. It was assumed that the air velocity did not appreciably affect the film thickness, and a parabolic velocity distribution existed. With these assumptions, the ratio of average velocity to surface velocity is two thirds. A calculation of the film thickness, by the formula shown in Fallah, Hunter, and Nash (*4*), gave the same result. The Reynolds number of the liquid film showed the film to be in the laminar state (Re_L = 167). The critical Reynolds number is about 1,200 for this system.

To show that the U drying tubes picked up all the moisture possible, air was drawn

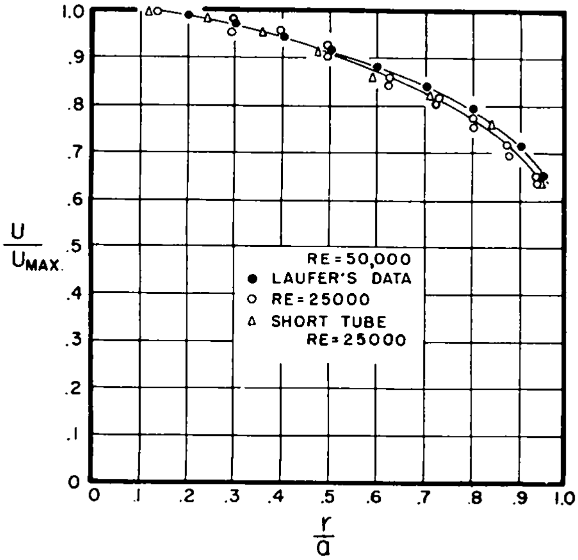

Fig. 2. Mean-velocity distribution.

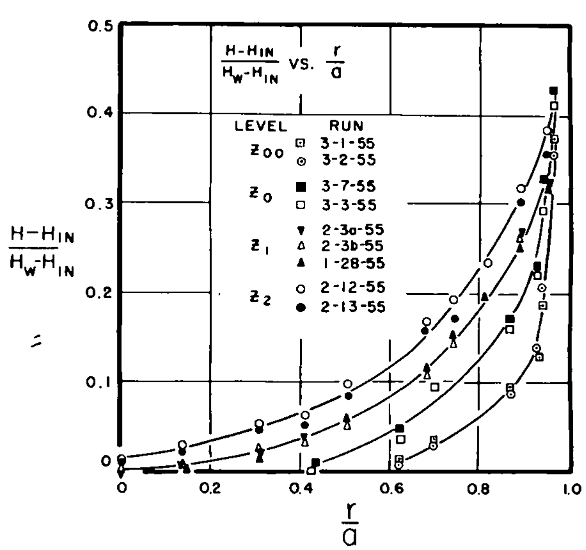

Fig. 3. Mean-concentration profiles.

Table 6

r/a	$\overline{u_r u_z}$	ϵ_m	$-\dfrac{\overline{u_r h} \times 10^{-3}}{H_w - H_{in}}$	$\epsilon \times 10^{-3}$	σ
0.05	0.04245	0.0209	0.7650	2.35	8.89
0.10	0.0846	0.01442	1.6446	2.915	4.946
0.15	0.1265	0.01078	2.725	3.351	3.217
0.20	0.1690	0.00973	4.2010	4.007	2.428
0.25	0.2105	0.00957	6.013	5.089	1.881
0.30	0.2525	0.00956	8.0971	6.398	1.494
0.35	0.2945	0.00982	10.39	7.605	1.291
0.40	0.3367	0.01004	12.574	8.368	1.199
0.45	0.3793	0.01032	14.498	8.717	1.183
0.50	0.4194	0.01053	16.30	8.467	1.243
0.55	0.4635	0.01072	18.237	8.062	1.329
0.60	0.5059	0.01085	20.251	7.843	1.384
0.65	0.5483	0.01092	22.29	7.324	1.490
0.70	0.5903	0.01097	24.379	6.577	1.667
0.75	0.6323	0.01062	26.448	5.88	1.806
0.80	0.6737	0.00966	28.425	5.088	1.898
0.85	0.008005	0.008005	30.699	4.566	1.753
0.90	0.00627	0.00627	32.998	4.183	1.4989
0.95	0.004192	0.004192	30.736	1.633	2.567
1.00					

through two U tubes in series at an air-flow rate corresponding to the maximum air-sampling rate used. There was no measurable weight increase of the second U tube.

RESULTS

The velocity distribution in the column as determined by the total head tube, which is shown in Figure 2, is compared with the results of Laufer (*10*). The data are tabulated in Table 1. The results have been put in the dimensionless form U/U_{max} vs. r/a.

The concentration profiles are plotted as $(H - H_{in})/(H_w - H_{in})$ vs. r/a and shown in Figure 3 and tabulated in Tables 2, 3, 4, and 5.* The curve shows the growth of the concentration profile down the tube. From these curves and the velocity profile, the correlation $\overline{u_r h}/(H_w - H_{in})$ was calculated as a function of the radius and is tabulated in Table 6. Equation (3) was used for this calculation. A plot of ϵ (eddy diffusivity for mass) vs. r/a is shown in Figure 4. The values of $\overline{u_r h}/(H_w - H_{in})$ and ϵ were calculated for level Z_2. [ϵ was calculated from Equation (4).] The method of calculation is shown in the Appendix. All values were computed by graphical methods.

From the velocity distribution in the tube, values of $\overline{u_r u_z}$ and ϵ_m were calculated, then tabulated and plotted in Table 6 and Figure 5, respectively. The ratio ϵ_m/ϵ is shown as a function of the radius in Figure 6. Equations (5) and (7) were used.

The rise in diffusivity along the center line is dictated by the fact that the diffusivity must tend toward infinity at the center line. In fact, the values of eddy diffusivity for mass and momentum have no meaning at the center-line region of the pipe because of the manner in which the diffusivities are defined. At the center line the terms $\partial H/\partial r$ and $\partial U/\partial r$ equal zero and the eddy diffusivities have no meaning. This explains the dashed portion of the curve on Figures 4 and 5. Also in Figure 6 the large rise of the curve of σ vs. r/a has little significance.

The results may be compared with the analogous heat transfer problem of a fluid flowing in a pipe with stepwise wall temperature. Isakoff and Drew (*8*) present data for the eddy diffusivity of heat calculated from temperature profiles in heating mercury flowing through a tube. These values are of the same order of magnitude as the values of ϵ calculated for mass transfer in the wetted-wall column. Johnson (*9*) has computed values of the turbulent Prandtl number for the boundary layer of a heated flat plate where the conditions are similar to the flow field in the column. In the portion of the flow of interest, he has found values between 0.8 and 1.1 as compared with values of σ between 1 and 2.

The local mass transfer was computed at the four levels by Equations (10) and (12). (*See* Appendix.) These values are tabulated in Table 7. The value of w_0 from Equation (12) is found by differentiation with respect to z of the curve on Figure 7. From this curve it may be seen that the local mass transfer rate is approximately constant over the range

*Tables 2 through 5 have been deposited as document 4793 with the American Documentation Institute, Photoduplication Service, Library of Congress, Washington 25, D. C., and may be obtained for $1.25 for photoprints or 35-mm. microfilm.

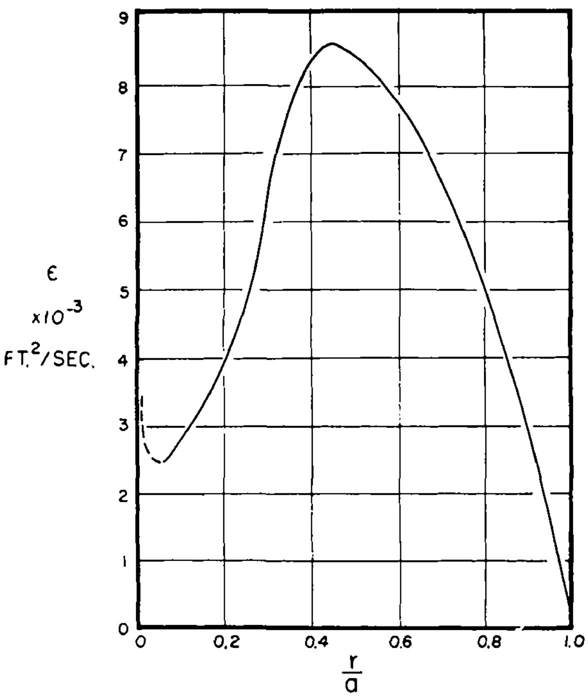

Fig. 4. Eddy diffusivity for mass vs. r/a. ←

Fig. 5. Eddy diffusivity for momentum vs. r/a. →

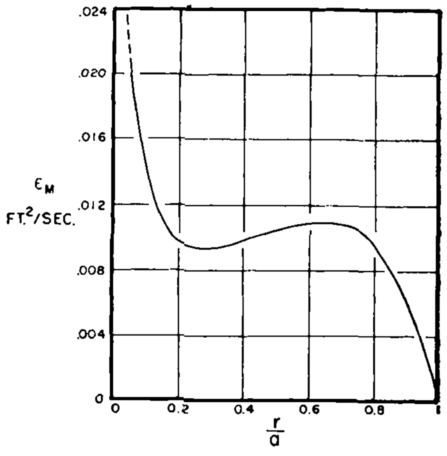

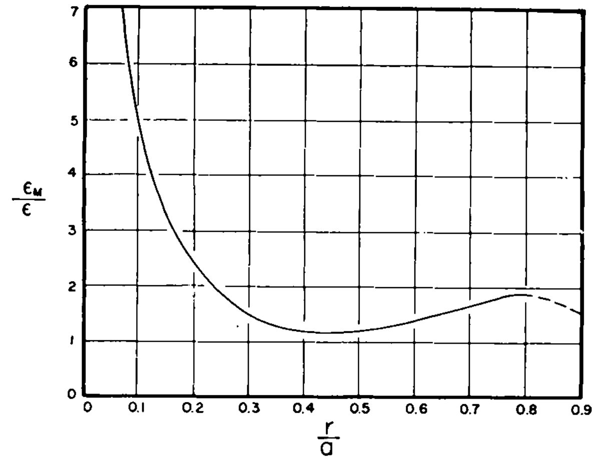

Fig. 6. Ratio of eddy diffusivity of momentum to mass vs. r/a.

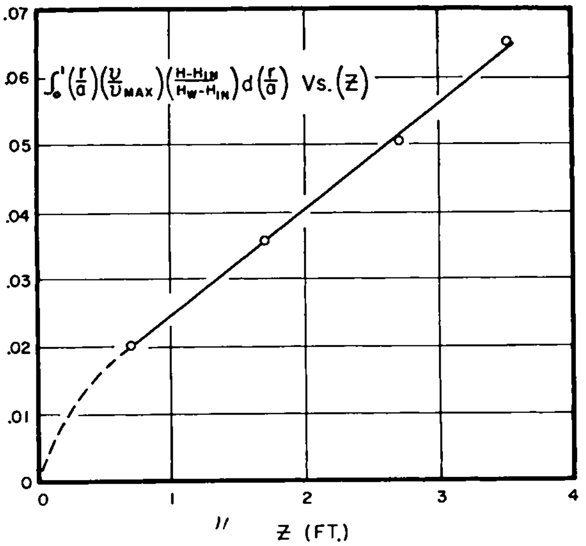

Fig. 7. Local mass transfer vs. column height.

measured. It can readily be seen that the rate becomes much higher near the inlet of the tube, where the concentration gradients are very much steeper.

CONCLUSIONS

A wetted-wall column has been constructed which produces a falling film essentially free from rippling. Special care has been taken to produce a fully developed turbulent profile of the air, which was measured and compared with the data of Laufer (*10*). The concentration profiles were measured at various distances downstream of the inlet. From these data the correlations $\overline{u_r u_z}$, $\overline{u_r h}$, and the eddy diffusivity for mass and momentum and their ratio were calculated. The local mass transfer was calculated at the various levels.

From the concentration profiles it is readily seen that many of the discrepancies in the literature concerning mass transfer data result from failure to consider entrance effects. Previous data have been correlated by the evaluation of the coefficients and exponents of a dimensionless equation, in which an over-all coefficient is expressed. Since the length of the column enters as a parameter of the problem, each system will have its own specific constants in the dimensionless equation, depending on the dimensions of the column. From the curve in Figure 7, it can be seen that the mass transfer rate does not become constant until the downstream distance has reached about six diameters.

TABLE 7. LOCAL MASS TRANSFER RATE COMPUTED FROM EQUATION (10)

$$w_{Z_{00}} = (0.002562)(H_w - H_{in})$$
$$w_{Z_0} = (0.002450)(H_w - H_{in})$$
$$w_{Z_1} = (0.002733)(H_w - H_{in})$$
$$w_{Z_2} = (0.002609)(H_w - H_{in})$$

From the slope of the curve (shown in Figure 13), the local mass transfer rate may be computed by Equation (12).

$$w = (0.002587)(H_w - H_{in})$$

NOTATION

- a = radius of tube (measured to interface) (0.1383 ft.)
- e_1 = outside diameter of probe (0.0655 in.)
- e_2 = inside diameter of probe (0.0451 in.)
- E = displacement of probe toward region of higher velocity
- h = humidity fluctuation—defined by the equation $H' = H + h$; *Note:* $\bar{h}$(mean value of h) = 0
- H = mean humidity, lb. H_2O/lb. dry air

Subscripts

- in = inlet humidity of air
- w = humidity of air at the wall in equilibrium with the water on the wall

- H' = instantaneous humidity
- P = pressure, lb./sq. ft.
- dP/dZ = pressure drop along axis of tube [mean value 0.02898 lb./(sq. ft.)(ft.)]
- r = distance from center line, ft.
- Re = Reynolds number = $2U_{max}\,a/\nu$
- Re_L = Reynolds number = $4\Gamma/\mu$
- t = time, sec.
- T = temperature, °K.
- u = velocity fluctuation—defined by the equation $U' = U + u$; *Note:* $\bar{u}$(= mean value of u) = 0 (Reynolds restriction)
- U = mean velocity, ft./sec.

Subscripts

- θ = azimuthal direction
- Z = along center line of tube
- r = in radial direction
- max = maximum velocity—corresponds to center-line velocity (mean value 15.6 ft./sec.)

- L = liquid velocity
- U' = instantaneous velocity
- w = local mass transfer rate, lb. H_2O/(sq. ft.)(sec.)
- W = mass flow rate, lb. dry air/sec.
- Z = distance along axis of tube from inlet of wetted section

Subscripts

- 00 = 8.56 in. from inlet (5.6 diam.)
- 0 = 20.56 in. from inlet (12.39 diam.)
- 1 = 32.56 in. from inlet (19.62 diam.)
- 2 = 42.31 in. from inlet (25.50 diam.)

- D = molecular diffusivity = sq. ft./sec. (1.626×10^{-4} sq. ft./sec.)
- ϵ = eddy diffusivity of mass, defined by Equation (4)
- ϵ_m = eddy diffusivity of momentum, defined by Equation (5)
- θ = azimuthal coordinate
- μ = viscosity of fluid, lb./(ft.)(sec.) for air, mean value 1.226×10^{-5}
- ν = kinematic viscosity of the air, sq. ft./sec. (1.626×10^{-4} sq. ft./sec.)
- Γ = flow rate of liquid = lb./(sec.)(ft.) of wetted perimeter
- ρ = density of air, lb. dry air/cu. ft. of air
- σ = defined as ϵ_m/ϵ

LITERATURE CITED

1. Corrsin, S., *Natl. Advisory Comm. Aeronaut., Tech. Note* 1864 (April, 1949).
2. ———, The Effect of Fluctuations in Chemical Concentration as Determined by a Sampling Probe, Course in Experimental Fluid Mechanics, The Johns Hopkins University, Baltimore, Md.
3. Emmert, R. E., and R. L. Pigford, *Chem. Eng. Progr.*, **50**, 87 (1954).
4. Fallah, J., T. G. Hunter, and A. W. Nash, *J. Soc. Chem. Ind.* (*London*), **53**, 368 (1934).
5. Gilliland, E. R., and T. K. Sherwood, *Ind. Eng. Chem.*, **26**, 516 (1934).
6. Goldstein, S., "Modern Developments in Fluid Dynamics," Oxford University Press, New York (1938).
7. Hurd, C. W., K. P. Chesky, and A. H. Shapiro, *J. Appl. Mechanics*, **20**, 253 (1953).
8. Isakoff, S. E., and T. B. Drew, *Proc. General Discussion on Heat Transfer*, Institution of Mechanical Engineers, London (1951).
9. Johnson, D. S., Ph.D. dissertation, Johns Hopkins Univ., Baltimore, Md. (1955).
10. Laufer, John, *Natl. Advisory Comm. Aeronaut. Tech. Note* 2954 (June, 1953).
11. Linton, W. H., and T. K. Sherwood, *Chem. Eng. Progr.*, **46**, 258 (1950).
12. Macmillan, F. A., *J. Royal Aeronaut. Soc.*, **58**, 570 (1954).
13. Martinelli, R. C., *Trans. Am. Soc. Mech. Engrs.*, **69**, 947 (1947).
14. Pankhurst, R. C., and D. W. Holder, "Wind Tunnel Technique," Sir Isaac Pitnam and Sons, Ltd., London (1952).
15. Schlinger, W. G., and B. H. Sage, *Ind. Eng. Chem.*, **45**, 657 (1953).
16. Schrage, R. W., "A Theoretical Study of Interphase Mass Transfer," Columbia University Press, New York (1953).
17. Sherwood, T. K., and R. L. Pigford, "Absorption and Extraction," 2nd ed., McGraw-Hill Book Company, Inc., New York (1952).
18. Whitwell, J. C., *Ind. Eng. Chem.*, **30**, 1157 (1938).
19. Young, A. D., and J. N. Maas, *Rept. & Memo.* 1770, Great Britain Aeronautical Research Council (September, 1936).

APPENDIX

The general mass transfer equation for axisymmetric flow, based on Reynolds restrictions, the assumption of steady state, and constant physical properties, is given in reference *6* as

$$U_z \frac{\partial H}{\partial z} = \frac{1}{r}\frac{\partial}{\partial r} r\left[(-\overline{u_r h}) + D\frac{\partial H}{\partial r}\right] \quad (1)$$

Integrating this equation with respect to r and using the boundary conditions that

$$\overline{u_r h} = 0 \quad \text{and} \quad \frac{\partial H}{\partial r} = 0$$

at $r = 0$, one obtains

$$\overline{u_r h} = D\frac{\partial H}{\partial r} - \frac{1}{r}\int_0^r rU_z \frac{\partial H}{\partial z} dr \quad (2)$$

where

$$\int_0^r rU_z \frac{\partial H}{\partial z} dr = [H_w - H_{in}]U_{max}a^2 \cdot \int_0^{r/a} \left(\frac{r}{a}\right)\frac{U}{U_{max}}\frac{\partial}{\partial z}\left(\frac{H - H_{in}}{H_w - H_{in}}\right)d\left(\frac{r}{a}\right)$$

and

$$\frac{\partial H}{\partial r} = \frac{(H_w - H_{in})}{a}\frac{\partial}{\partial(r/a)}\left(\frac{H - H_{in}}{H_w - H_{in}}\right)$$

Equation (2) thus may be written

$$\frac{\overline{u_r h}}{[H_w - H_{in}]} = \left\{\frac{D}{a}\frac{\partial}{\partial(r/a)}\left(\frac{H - H_{in}}{H_w - H_{in}}\right) - \frac{U_{max}}{(r/a)}a \cdot \int_0^{r/a}\frac{r}{a}\left(\frac{U}{U_{max}}\right)\frac{\partial}{\partial z}\left(\frac{H - H_{in}}{H_w - H_{in}}\right)d\left(\frac{r}{a}\right)\right\} \quad (3)$$

A "transport coefficient" ϵ may be defined by $\epsilon(\partial H/\partial r) \equiv -\overline{u_r h}$. Thus

$$\epsilon = \frac{-\overline{u_r h}}{\frac{\partial H}{\partial r}} = -\frac{-\overline{u_r h}}{\frac{(H_w - H_{in})}{a}\frac{\partial}{\partial(r/a)}\left(\frac{H - H_{in}}{H_w - H_{in}}\right)} \quad (4)$$

A "momentum transport coefficient" ϵ_m may be defined as

$$-\overline{u_r u_z} \equiv \epsilon_m \frac{\partial U}{\partial r}$$

Thus

$$\epsilon_m = \frac{-\overline{u_r u_z}}{\frac{\partial U}{\partial r}} = \frac{-\overline{u_r u_z}a}{\left\{\frac{\partial}{\partial(r/a)}\left(\frac{U}{U_{max}}\right)\right\}U_{max}} \quad (5)$$

Finally, by definition, $\sigma = \epsilon_m/\epsilon$ = a "turbulent Schmidt number."

From the Navier-Stokes equation one may obtain

$$\int_0^r \frac{r}{\rho}\frac{dP}{dz} dr = r\left[-\overline{u_r u_z} + \nu\frac{\partial U_z}{\partial r}\right] + \text{constant} \quad (6)$$

When the boundary conditions

$$\frac{\partial U_z}{\partial r} = 0 \quad \text{and} \quad \overline{u_r u_z} = 0$$

at $r = 0$ are utilized, the constant is seen to be zero.

Thus

$$\overline{u_r u_z} = \frac{-a}{2\rho}\frac{\partial P}{\partial z}\left(\frac{r}{a}\right) + \frac{\nu}{a}U_{max}\frac{\partial}{\partial(r/a)}\left(\frac{U}{U_{max}}\right) \quad (7)$$

The local mass transfer rate may be written as follows:

$$w = \frac{\rho}{a}\int_0^a rU_z \frac{\partial H}{\partial z} dr \quad (8)$$

This has been shown equal to $\rho[D(\partial H/\partial r) - \overline{u_r h}]$ and values of N_0 may be found by graphical integration. In terms of dimensionless ratios,

$$\frac{U}{U_{max}}, \quad \frac{r}{a}, \quad \text{and} \quad \frac{H - H_{in}}{H_w - H_{in}},$$

Equation (8) becomes

$$w = \rho[H_w - H_{in}]U_{max}a \cdot \int_0^1 \left(\frac{r}{a}\right)\left(\frac{U}{U_{max}}\right)\frac{\partial}{\partial z}\left(\frac{H - H_{in}}{H_w - H_{in}}\right)d\left(\frac{r}{a}\right) \quad (9)$$

N_0 may also be calculated from Equation (1) written in the form

$$\int_0^a \frac{d}{dz}(rU_z H)\, dr = \int_0^a \frac{\partial}{\partial r} r\left[(-\overline{u_r h}) + D\frac{\partial H}{\partial r}\right] dr \quad (10)$$

By Leibnitz rule, with $\overline{u_r h} = 0$ taken at the wall,

$$\rho\frac{d}{dz}\int_0^a rU_z H\, dr = aw$$

Thus

$$w = \frac{1}{a}\frac{d}{dz}\int_0^a \rho r U_z H\, dr \quad (11)$$

And at the wall

$$w = D\frac{\partial H}{\partial r}\cdot\rho$$

Letting

$$r = \frac{r}{a}\cdot a,$$

$$H = \left(\frac{H - H_{in}}{H_w - H_{in}}\right)(H_w - H_{in}) + H_{in}$$

$$dr = ad\left(\frac{r}{a}\right) \qquad U_z = \frac{U_z}{U_{max}}\cdot U_{max}$$

and simplifying, one may write Equation (11) as

$$w = aU_{max}(H_w - H_{in})\rho\frac{d}{dz} \int_0^1 \left(\frac{r}{a}\right)\left(\frac{U}{U_{max}}\right)\left(\frac{H - H_{in}}{H_w - H_{in}}\right)d\left(\frac{r}{a}\right) \quad (12)$$

This equation permits the calculation of w by, first, a graphical integration, which is a smoothing effect, then a differentiation.